Tuijin Jishu/Journal of Propulsion Technology
ISSN: 1001-4055
Vol. 45 No. 3 (2024)

Investigation on the Effect of Leading-Edge Tubercles of Multitudinal Airfoils at Low Reynolds Number

V. T. Gopinathan [1]*, R.Saravanan[2], M.Ganesh[3]

[1],[3]Associate Professor, [2]Assistant Professor, Department of Aeronautical Engineering, Hindusthan College of Engineering and Technology, Coimbatore, India.

Abstract: On the observation of biomimetic of Humpback Whale (HW) flipper, the aerodynamic performance characteristics are explored. The flipper of HW has rounded leading edge (LE) tubercles and tapered trailing edge configuration. The tubercles have excellent flow control characteristics at the post stall region. Aerodynamic characteristics of NACA airfoils such as NACA 0015 and 4415 with LE tubercles are experimentally and numerically investigated at the Reynolds number about Re=1.83×10^5. The modified airfoils (BUMP 0015 and 4415) are designed with the amplitude to wavelength ratio (η) of 0.05. The numerical simulation over the modified airfoils shows that, the flow separation is less in peak region and high in trough region because of the counter rotating vortices at high Angle of Attack (AoA). Hence the tubercles effectively suppress the stall through the optimized flow separation behaviour. The important pressure distribution variation over mid, trough and peak regions of modified airfoils are computed for different AoA using a subsonic wind tunnel facility. These values are compared with pressure distribution of baseline airfoils experimentally. The Co efficient of Lift (C_L) and Co efficient of Drag (C_D) also computed for modified and baseline airfoils to enhance the aerodynamic performance. The stall delay phenomenon is observed through the outcome of the analytical results that insists on peak, trough and medial region. Comparison of Pressure Coefficients (C_P) and C_L, C_D between the base line and modified airfoil reveals the momentum transfer characteristics of tubercles.

Keywords: Bio-inspired surfaces, Stall, Wind tunnel testing, L/D optimization, CFD

Nomenclature

A	=	Amplitude
α	=	Angle of attack
Δc	=	Chord length variation
C_L	=	Coefficient of lift
C_D	=	Coefficient of drag
C_p	=	Coefficient of pressure
$\bar{c}$	=	Mean chord
η	=	A/ λ
λ	=	Wavelength
LWS	=	Lower surface of airfoil
UPS	=	Upper surface of airfoil
Z	=	Span wise ordinate

I. Introduction

AERODYNAMICISTS, in academics and industry progressively investigate the flow field towards mastery of proficiency in flow control. Numerous studies supported that Humpback Whales (Megaptera novaeangliae) maneuverability trigger to implement flippers composition by the idea of examining leading edge tubercles on airfoils in order to suggest that lift enhancement devices, hence delaying stall through admit flow remains attached for a larger range AoA. Fish and Battle (1995) describe about morphology of HW flipper, that have large aspect ratios where large-scale tubercles located along the LE, the thickness ratio ranges from 0.2 to 0.28 of the chord length and reported the amplitude of the tubercles changes from 2.5% to 12% of the chord length and the wavelength ranges from 10% to 50% of the chord. Miklosovic et al. (2004) reported that scalloped leading edge of the flipper aids to delay stall by providing higher lift at higher incidence angles and to upgrade the post-stall characteristics by maintaining higher lift with lower drag.

A large eddy simulation study undertaken by Skillen et al. (2013) contributed that undulated leading edge of NACA 0021 airfoil has got 36% gain in mean lift and 25% reduction of mean drag. They explored the mechanism involved in reduction of the size of separation zone. Karthikeyan et al. (2014) experimentally studied the effect of wavy LE of NACA 4415 at low Reynolds number. Their 2-D PIV and oil flow resulted that the tubercles are very much effective in post-stall conditions compared to baseline airfoils. They also found that the size of recirculating zone at the downstream of airfoil. The implementation of Prandtl's lifting line theory over NACA 0021 wing with introduction of new tubercle parameter called "phase of the tubercle" has been studied by Bolzon et al. (2016). It is found that the phase of tubercles has huge effect on the lift coefficient, induced drag coefficient and lift to induced drag coefficient, while wavelength had least effect.

Rostamzadeh et al. (2014) experimentally and numerically tested the effect of tubercles on the flow structure over full span modified NACA 0012 wing in transitional flow regime. They reported that the presence of vortices is unfavorable to wing's performance in pre-stall conditions. Whereas the performance is advantageous in post-stall where the primary and secondary vortices delayed the flow separation by enhancing the momentum transfer. Favier et al. (2012) investigated the effect of wavy leading edge over NACA 0020 wing profile at low Reynolds number. They studied the influence of streamwise vortices on the boundary layer separation. The effect of tubercles varies depending upon the airfoil profiles. By finding the optimized values of amplitude and wavelength of tubercles, the pre-stall, stall and post-stall performances can be very much improved. The performance of wing can be improved by having tubercles on the leading edge. They act as a passive flow control device which delays the stall angle, thereby the lift is increased with reduction in drag. The streamwise vortices modifies the boundary layer and reduces both tip vortex strength and spanwise flow was examined by Frank.E.Fish et al (2011).

Johari et al (2007) carried out a systematic experimental study on NACA 63_4-021 airfoil with tubercles of different combinations of amplitude and wavelengths. The results from these experiments show that the airfoil incorporated with leading edge protuberances generates 50% higher lift with no drag penalty in the post stall region compared to baseline airfoil. While amplitude of the protuberance exhibited a notable effect on the performance of the airfoil, the wavelength had very little influence. Alessandro Corsini et al. (2013) exhibits the numerical investigation into the effects of a sinusoidal leading edge fitted to NACA 0015 and NACA 4415 profiles were analyzed using Open FOAM software and reported that the modified airfoil performance recovers earlier during stall and has 30% increment of lift at post-stall for unsymmetrical modified airfoil. An experimental investigation had been undertaken by Kristy.L.Hansen (2011) is to determine the influence of tubercles on the performance of NACA 65-021 and NACA 0021 airfoils. It was found that the lift performance in the post-stall regime has increased.

M.M.Zhang et al. (2013) examined the effects of sinusoidal leading-edge protuberances on two dimensional full-span airfoil aerodynamics were investigated at a low Re of 5.0×10^4 and indicated that in boundary-layer separation control, the function of protuberances is very similar to a low-profile vortex generator to a certain degree. The effect of the airfoil thickness variation in the wavy leading edge was examined for NACA 0020 and NACA 0012 by Adson et al. (2016) . The result revealed that increase in airfoil thickness causes aerodynamic

deterioration at pre-stall regime for wavy leading-edge airfoil. The computational investigation conducted by Pedro et al. (2008) [14] showed the existence of streamwise vortices that increased vorticity along the downstream of the flow and reduction in tip vortex strength. Theoretically, the delayed separation of flow in some regions due to the presence of tubercles has been predicted by Van Nierop et al. (2008).

II. Numerical Methodology

A. Airfoil Geometry

NACA 0015 and NACA 4415 airfoils are selected as the baseline geometries. These profiles are used to create airfoils with sinusoidal leading edge which are named as BUMP 0015 and BUMP 4415. The governing geometric parameters that affect the performance of tubercles are wavelength (λ), amplitude (A) and the ratio of amplitude to wavelength (A/λ) represented as η. They retains high-priority in the design perspective of tubercle proceedings. The mean chord length of all profiles used in the present study is kept constant. The spanwise ordinates for the variable chord length is given by henceforth wave equation,

$$c(Z) = A\cos\left(\frac{2\pi Z}{\lambda}\right) + \bar{c}$$

The variation in chord length (Δc) along span wise direction is presented in Figure1. The modified airfoils have mean chord length c=100 mm. The modified airfoils have a LE tubercles profile along the span wise direction with amplitude A=0.5c and wavelength of λ=0.025c. The ratio of amplitude to wavelength is 0.05. The graph signifies span wise ordinates (z) and variation in chord length (Δc) on x axis and y axis respectively.The CAD models of modified airfoils are shown in Figure 2.

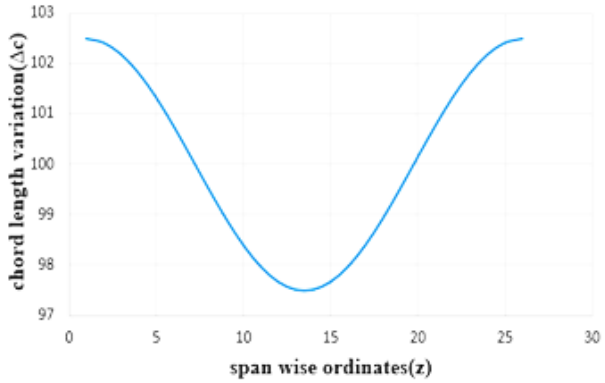

Figure 1. Chord length variations along the span wise ordinates

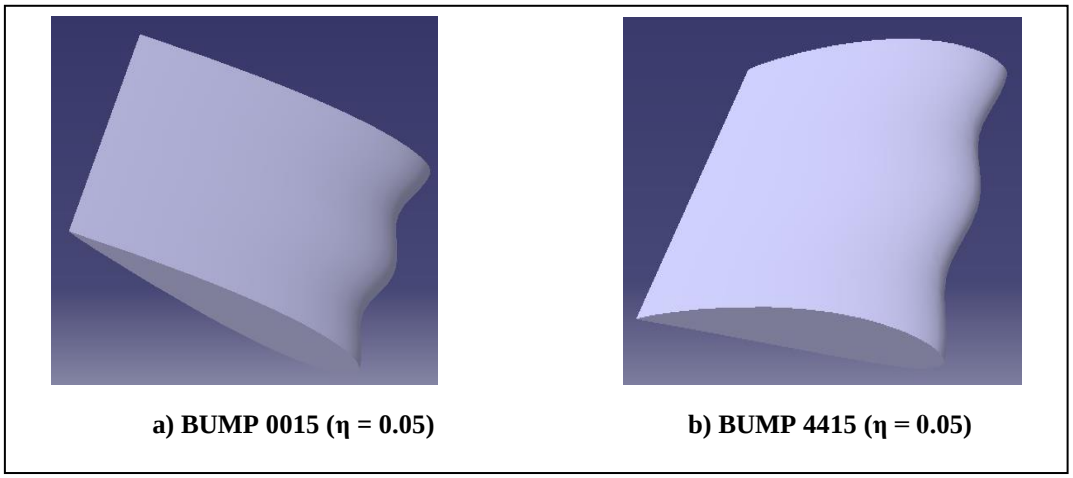

a) BUMP 0015 (η = 0.05) **b) BUMP 4415 (η = 0.05)**

Figure 2. CAD model of modified airfoil profiles

B. Computational Meshing and Numerical Simulation

Meshing is carried out using unstructured grid with tetrahedral elements. Naming the airfoil such as upper and lower surface, upper surface leading edge, lower surface leading edge and end is essential for meshing. It helps to initialize the mesh element size. The pre mesh parameters are global mesh, shell mesh, volume mesh and prism layer parameters given in meshing structures. The y^+ value for all the simulations are maintained below 3. The total number of elements which includes surface and volume elements, for NACA 0015, NACA 4415, BUMP 0015 and BUMP 4415 are $1.3x10^6$, $1.4x10^6$, $1.1x10^6$ and $1.1x10^6$ respectively. Generation of mesh with prism layers over airfoil is shown in Fig.3.Numerical analysis is done by using FLUENT tool to catch the flow over the full span base line and protuberance modelled airfoils. The turbulence model SST K- ω has been used to solve steady state compressible Reynolds averaged Navier-Strokes equation (RANS).

$$\rho\left(\frac{\partial U_i}{\partial t}+U_k\frac{\partial U_i}{\partial x_k}\right)=-\frac{\partial P}{\partial x_i}+\frac{\partial}{\partial x_i}\mu\left(\frac{\partial U_i}{\partial x_j}\right)+\left(\frac{\partial R_{ij}}{\partial x_j}\right)$$

Where R_{ij} is Reynolds stresses, U,p,ρ represents the mean flow quantities. Extent of computational domain is spherical domain of 20 chord length. Boundary conditions are two sides of domain as wall while the remaining domain surface will be pressure far field and the interior of the domain named as fluid

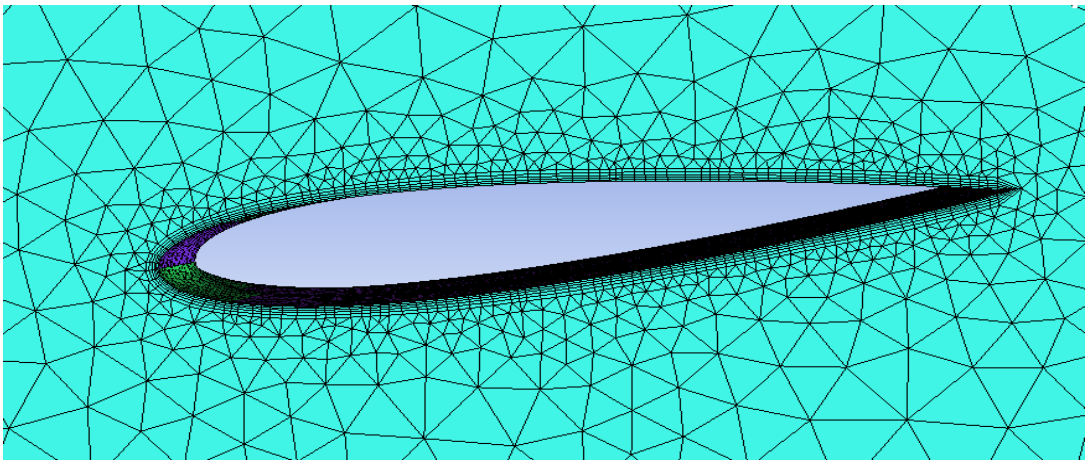

Figure 3. Generation of mesh with prism layers

III. RESULTS & DISCUSSION

To investigate the effect of tubercles, the baseline airfoils and the modified airfoils were simulated with same Reynolds number. The numerical simulation was carried out at the angles of attack ranging from 0° to 20°. The effect of tubercles was identified based on aerodynamic coefficients, coefficient of pressure with the aid of streamline patterns over the airfoils and velocity vector contours simulated at leading edge of modified airfoils.

A. Streamline patterns

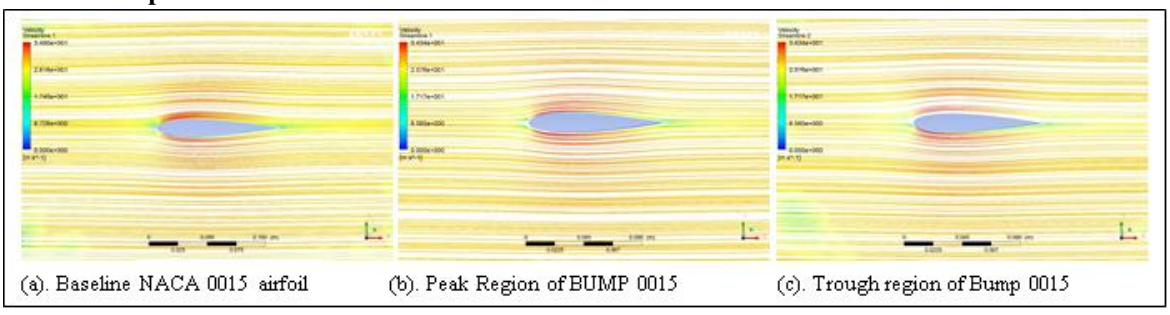

Figure.4 Streamline fields of airfoil at different regions at AoA, α = 0°

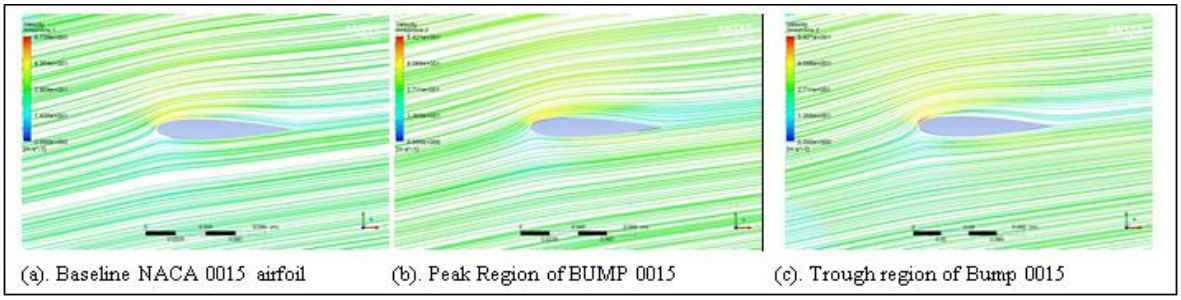

Figure.5 Streamline fields of airfoil at different regions at AoA, α = 10°

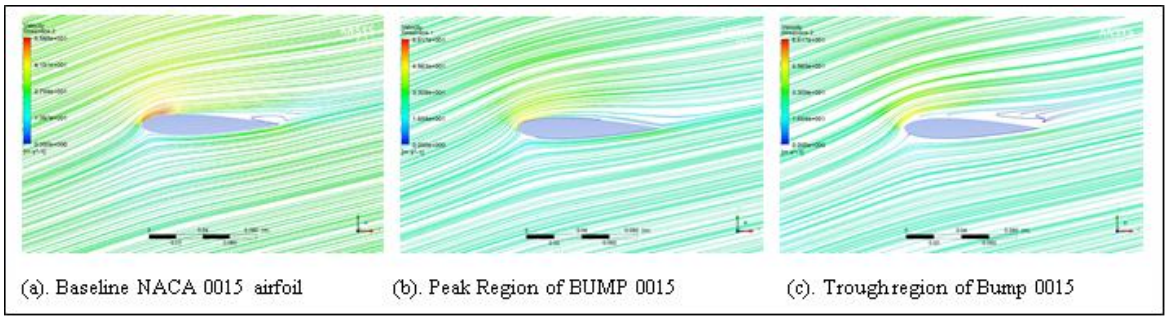

Figure.6 Streamline fields of airfoil at different regions at AoA, α = 15°

To identify the basic mechanism and flow separation behavior of airfoils with LE tubercles, the amplitude to wavelength ratio 0.05 is selected. Streamline patterns are presented for baseline and modified airfoils at AoA of α =0°, α=10°, α=15°. The streamline patterns depicted in Fig.4 represent the flow over symmetrical baseline airfoils and modified airfoils with η = 0.05. The flow is attached over the surface of NACA 0015 at AoA is 0º. As the AoA increases to α =10º, the flow separation starts to appear on the suction side of the airfoil. At α =15°, the recirculating flows could be observed. The flow separation point occurs at one-third of the chord from the leading edge (Fig. 4). The laminar separation bubble at the leading edge of baseline airfoil starts bursting during the stall which increases the drag. In the modified airfoils, flow has attached in both peak and trough regions at low AoA regime. Along the trough plane, the flow separates from LE. The flow separation control along the peak region is interesting to note. The BUMP 0015 employed with η = 0.05, has got delayed separation point in the peak region and the flow is separated near the leading edge of the airfoil in trough region at 15º (Fig. 6). Though the trough region faces earlier separation of flow, the flow over peak region provides additional lift and increases the range of stalling angle compared to baseline airfoil. At post-stall angles of attack, airfoils experience a reduction in lift due to flow separation. The streamwise vortices formed in between the trough region exchanges the momentum into the flow. The circulation of flow in downstream direction increases. As a result, the flow tends to attach with the upper surface of the airfoil yielding large increase in lift.

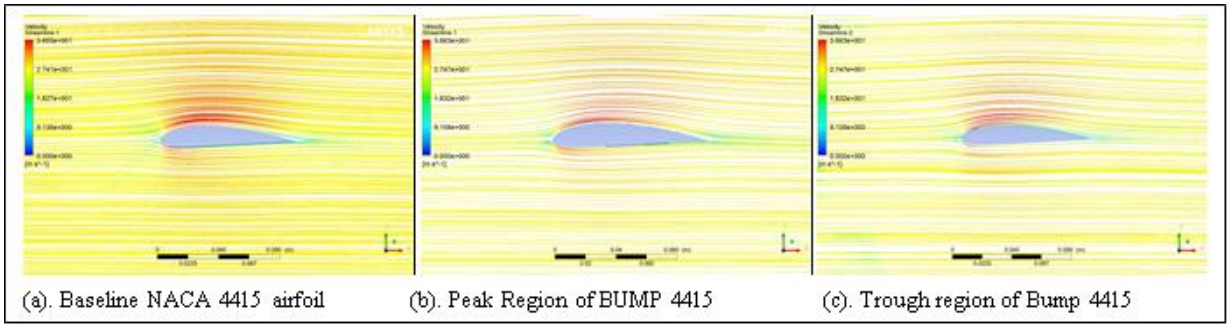

Figure.7 Streamline fields of airfoil at different regions at AoA, α = 0°

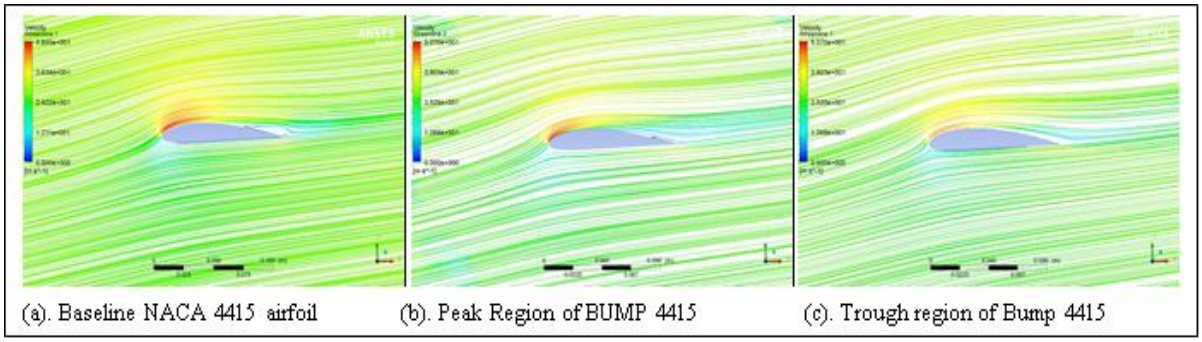

Figure.8 Streamline fields of airfoil at different regions at AoA, α = 10°

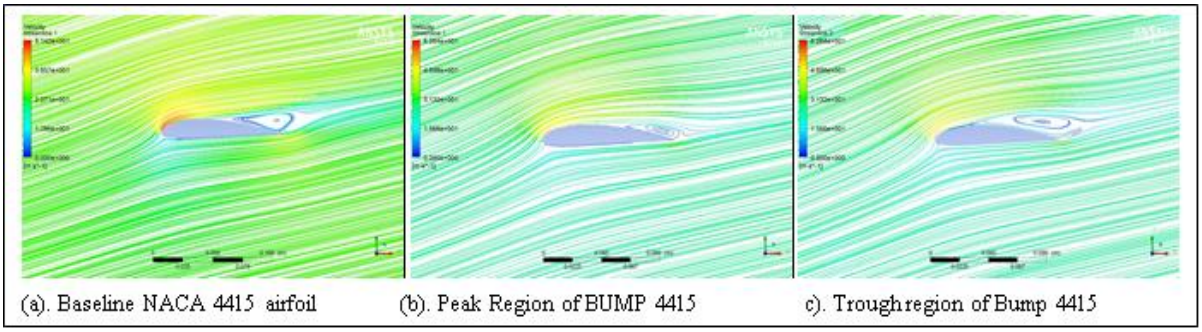

Figure.9 Streamline fields of airfoil at different regions at AoA, α = 15°

Above figures depicts the streamline flow patterns over cambered airfoil where NACA 4415 serves as the baseline profile and BUMP 4415 airfoil (η = 0.05) is modified profile. The flow separation can be detected at α =0° for baseline cambered aerofoil.As AoA increases, the flow separation point move towards the LE of the airfoil. In modified airfoils, the flow has got enough amount of energy to flow over the surface of the airfoil in both peak and trough regions without separation at low AoA, as shown in Figure.8. But at higher AoA, the flow tends to attach in the peak region compared to trough region. At α = 15°, the laminar separation bubble is formed in the downstream of airfoil at peak region. The trough region of BUMP 4415 (η = 0.05) airfoil experiences a deep stall condition. A main vortex covers the majority of the suction side with a gradual formation of secondary vortex behind it. As the AoA gets increased, the separation point in trough region nears the stagnation point. However, the flow stills stays attached in the peak region along the surface for more than half of the chord as shown in Figure.9. Thus, the tubercles help in increasing the flow attachment area at higher angles of attack with improvement in aerodynamic characteristics and better stall characteristics.

B. Effect of Tubercles on Pressure Distribution

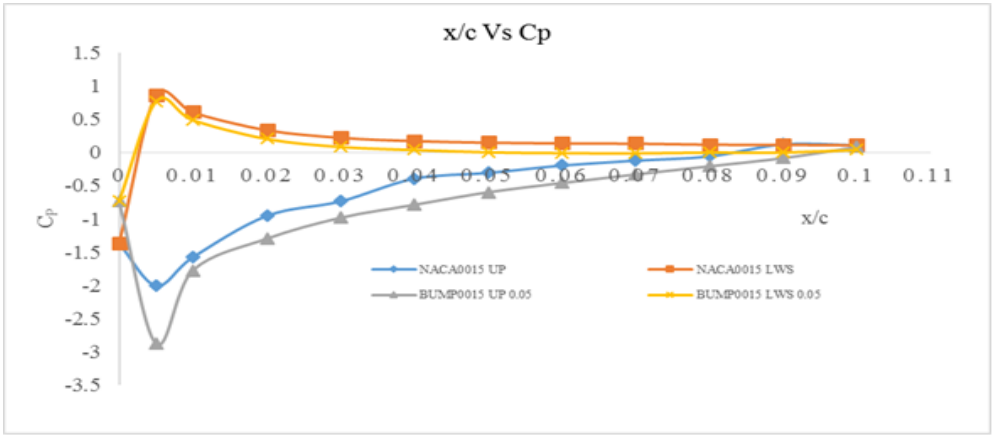

Figure.10.Pressure distribution of baseline and modified symmetric airfoil at α =10°

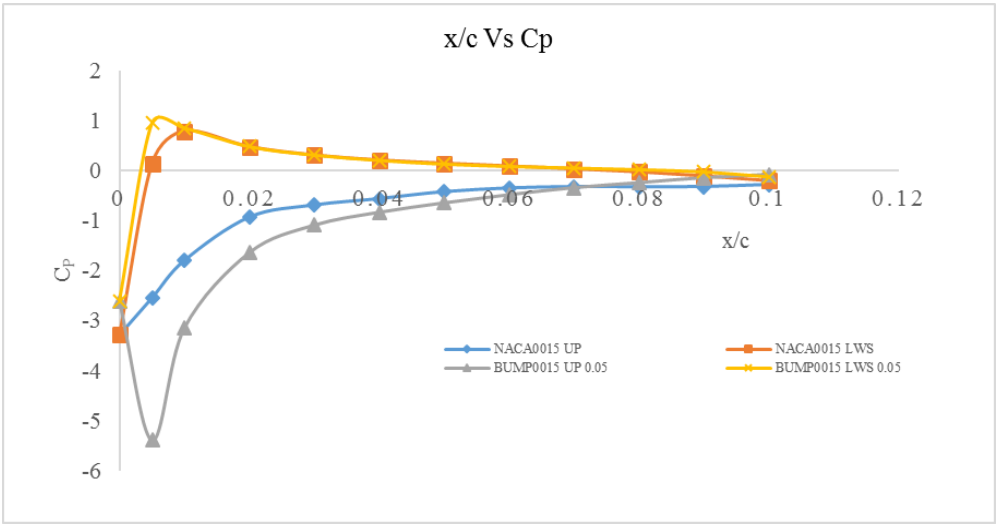

Figure.11. Pressure distribution of baseline and modified symmetric airfoil at α =15º

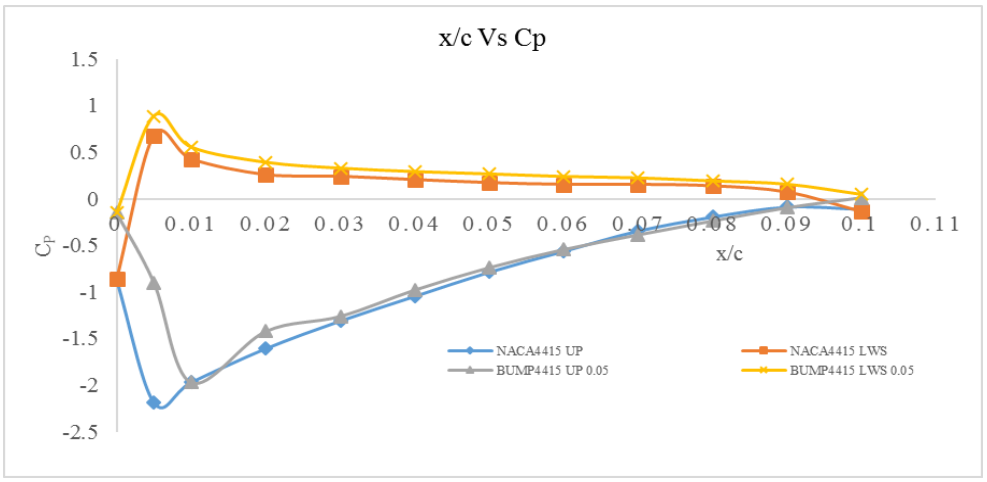

Figure.12. Pressure distribution of baseline and modified unsymmetrical airfoil at α =10º

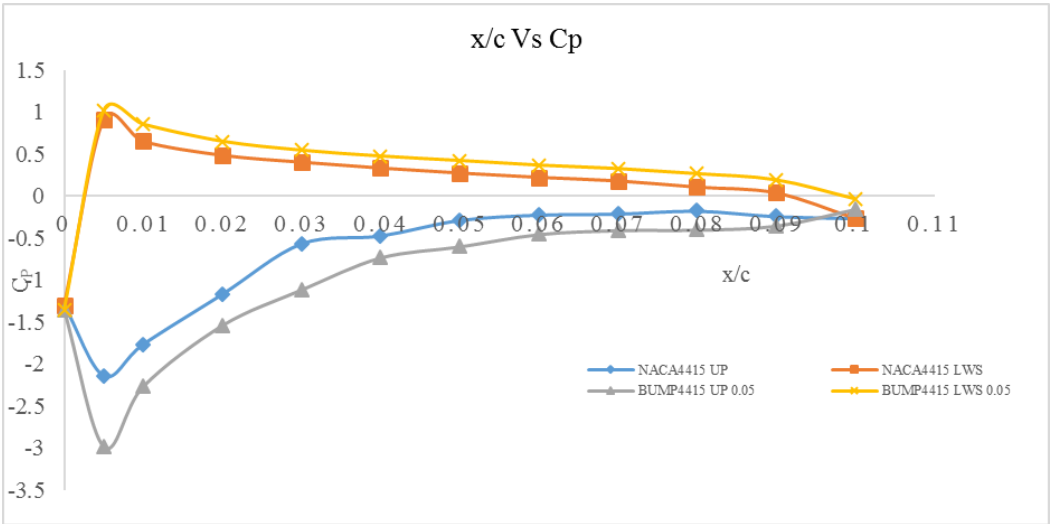

Figure.13. Pressure distribution of baseline and modified unsymmetrical airfoil at α =15º

The chord wise pressure distribution for baseline air foils and modified air foils are plotted in the above graphs. Analysis of the surface pressure distribution allows identification of the point at which the initiates for each cross section. In the baseline airfoil, the Cp achieves a minimum value near the leading edge and after the peak value, the Cp increases along the downstream creating strong adverse pressure gradient. This causes the boundary layer to separate from the top surface. The most negative values of the peak pressure developed over the suction surface of the BUMP 4415 aerofoil at $\alpha = 10^{o}$, is associated with the trough cross section. With the addition of the tubercles, the maximum suction peak almost the same, the subsequent rate of increase of Cp is less. So the adverse pressure gradient over the aerofoil is decreased and hence the stall is delayed.

IV.Experimental Technique

In experimental investigation, the same baseline airfoils (NACA 0015 ,4415) and modified airfoils (BUMP 0015,4415) are used with the span of cavity molding is utilized for making an airfoil, the patterns using teak wood was made for baseline airfoils and modified airfoils. It is desirable to have highest possible filling speed during filling phase. The glass fiber and epoxy resin employed to make the models. Utilizing cavity molding manufacturing process, the requisite airfoils were shaped and created. The model is allowed to cool and proceeded to finishing process. By drilling 1.4mm diameter hole on the surface for pressure tappings fixation. According to the x/c values the pressure tappings were fixed on upper and lower surfaces of airfoils.

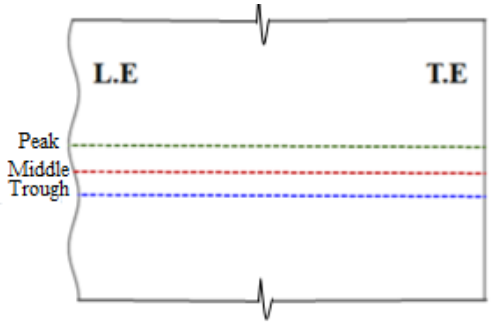

Figure.14. Schematic diagram of peak, middle and trough region of tubercles.

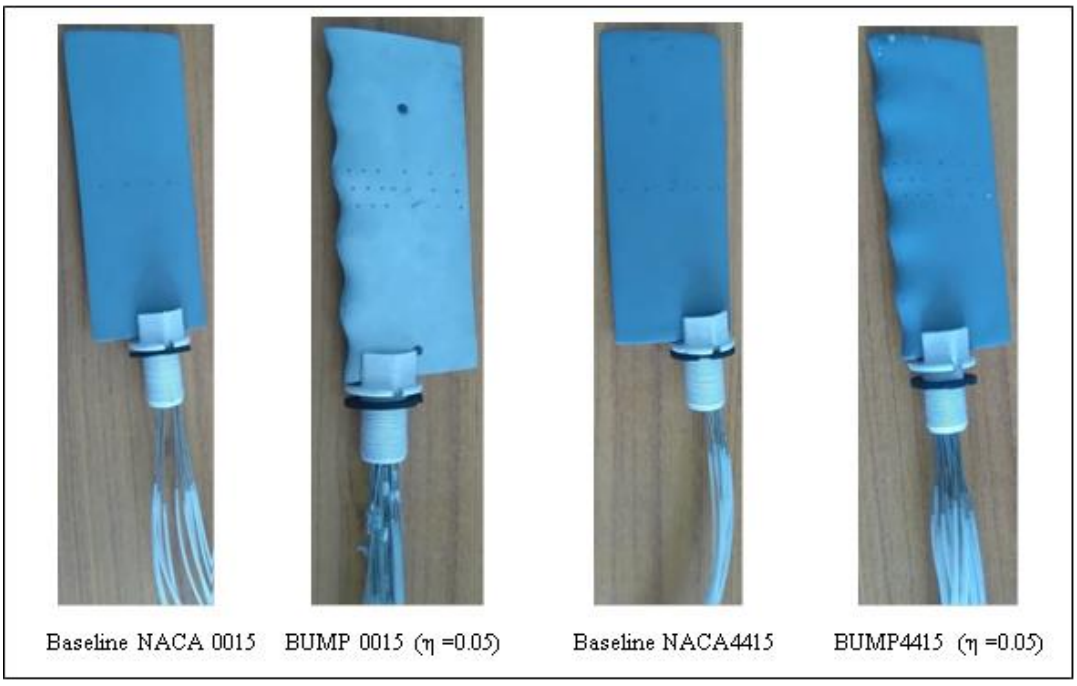

Figure.15. Photographs of baseline and modified airfoils with LE tubercles

On the baseline airfoils, the pressure tappings were placed at the ratio y/b=0.5. While for the modified airfoils, the ratio provided for the peak, middle and trough regions to fitting pressure tappings. Steel tube has employed for fitting measurable pressure tappings. After the fixation of tappings, the upper and lower surfaces have combined utilizing araldite. Using subsonic wind tunnel, the experimental validation was carried out. The employed wind tunnel is suction type with an axial flow fan driven by a 2880 rpm which is 15 HP 440 volts 50 cycles 3 phase AC motor. The total length of the wind tunnel is about 6.0 m. The axial flow fan and the duct is 0.9 m long. The maximum height is about 1.2 m. The test section of 30 cm * 30 cm cross section and 100 cm length with thick Plexiglas window. The model is mounted vertically and the pressure tappings tube is elongated and connected through 1.5 mm and 2.5 mm tubes to the manometer measurement tubes.

(a) **(b)**

Figure.16. Photographs of a) Front mounting of airfoil in test section, (b) Top view on mounting of airfoil in test section

A. Experimental analysis

The initial readings of manometer were noticed after mounting. The wind tunnel is allowed to flow 27.5 m/s. The change in manometer readings were noted for various AoA in the range of 0 ° to 21° for baseline and modified airfoils. Using coefficient of pressure formula, the pressure distribution for upper and lower surfaces was found out.

Coefficient of pressure, $C_P = \left(\frac{P_i - P_s}{P_o - P_s} \right)$

Where,

P_i = Pressure from pressure tappings (N/m^2),

P_s = Static pressure or reference pressure (N/m^2),

P_o = Total pressure (N/m^2),

Experimental pressure distribution

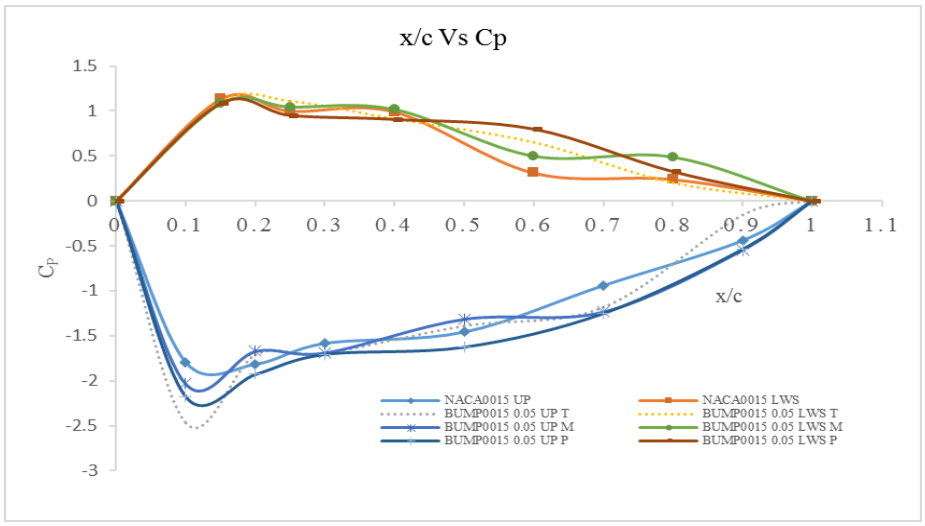

Figure.17. Experimental pressure distribution of baseline and modified Symmetric airfoil at α =10º

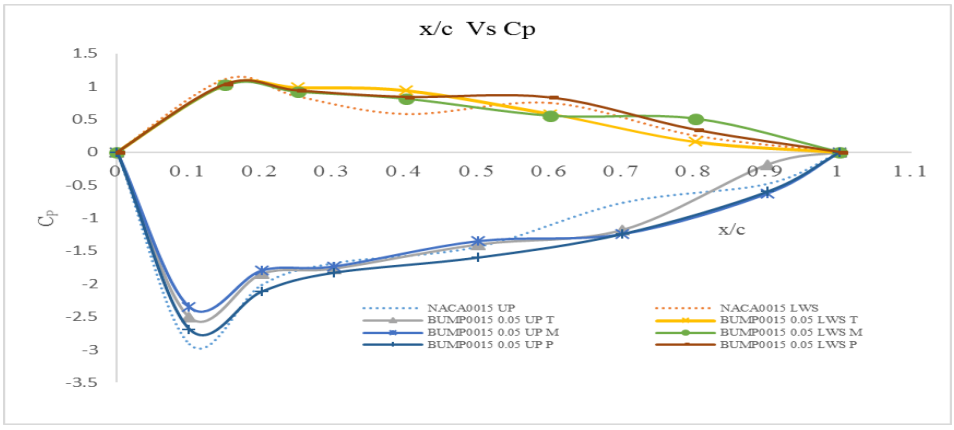

Figure.18. Experimental pressure distribution of baseline and modified Symmetric airfoil at α =14º

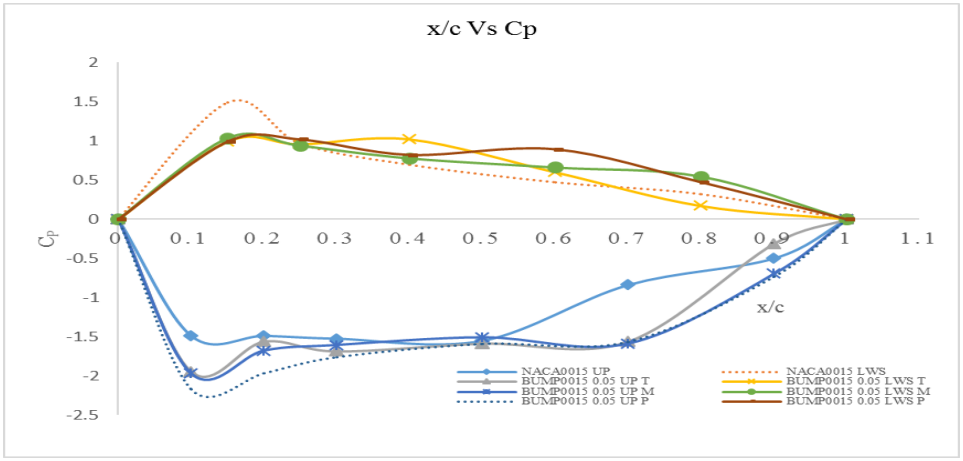

Figure.19. Experimental pressure distribution of baseline and modified Symmetric airfoil at α =18º

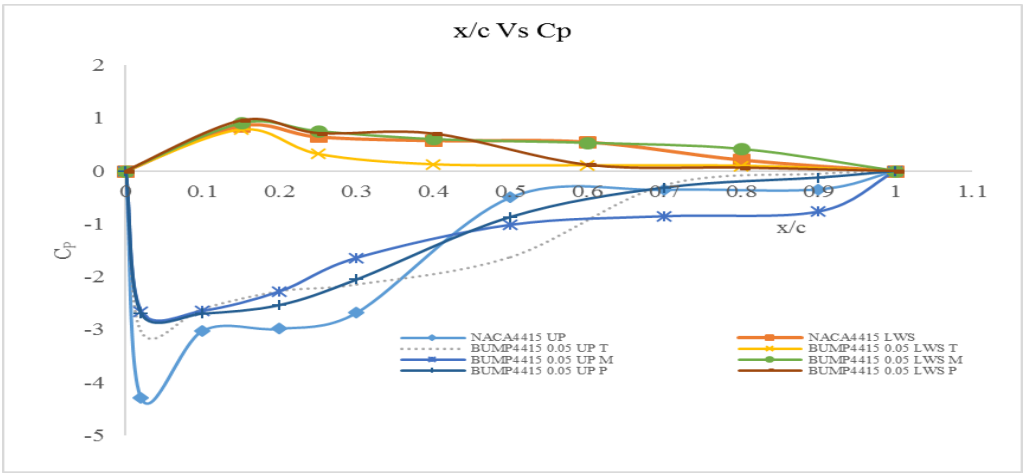

Figure.20. Experimental pressure distribution of baseline and modified Unsymmetrical airfoil at α =10º

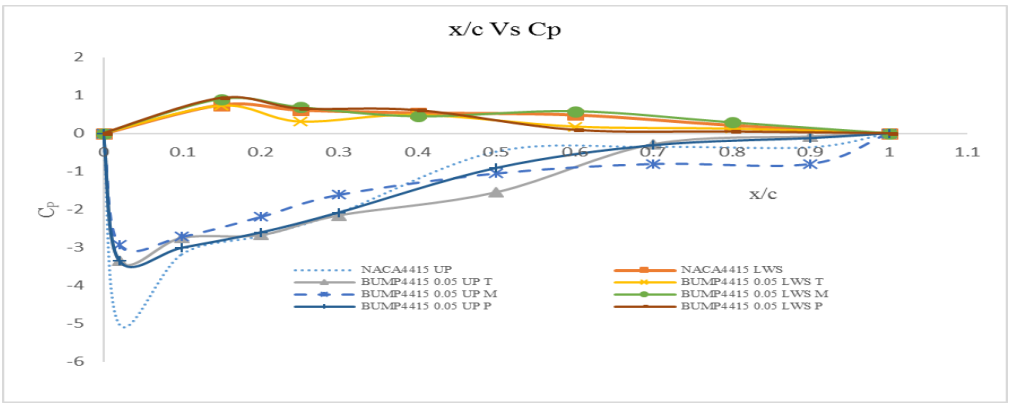

Figure.21. Experimental pressure distribution of baseline and modified Unsymmetrical airfoil at α =12º

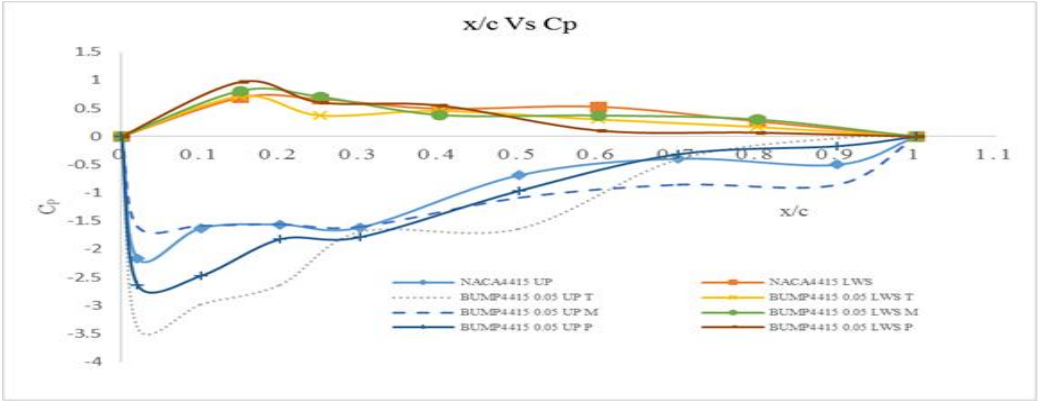

Figure.22. Experimental pressure distribution of baseline and modified Unsymmetrical airfoil at α =15º

As the tappings were positioned on the suction and pressure side for the baseline and modified airfoils, the pressure distribution is elucidated. Extreme concern was taken to measure the pressure distribution readings in peak, trough and mid region modified airfoils. The chord wise pressure distribution shows the existence of span wise variation in pressure by means of effective aerodynamic characteristics. The computational and experimental validation for pressure distribution shows the similar effect of tubercles over baseline and

modified profiles (Figure.10. & Figure.17.). Towards the comparison of NACA0015 and BUMP0015, at α=10° utmost negative pressure appearing in trough region on the suction surface and rate of increases of adverse pressure gradient is less in downstream (static pressure decreases). Whereas the pressure distribution in middle region higher than trough and lower than peak region. By the cause of decrease in dynamic pressure, the pressure distribution of peak, trough and middle region is high compared to baseline airfoil and no significant distribution of pressure-on-pressure side nearer to the leading edge shown in Fig.17. At α=14°, the baseline airfoil possesses high negative pressure distribution compare to peak, trough and mid region on suction surface as a result of dropping of static pressure in downstream of airfoil. On pressure side, the positive pressure distribution of modified airfoil is inferior to baseline airfoil although no indicative pressure distribution on peak, trough and middle at leading edge shown in Fig.18. At α=18° maximal negative dispersion of pressure in peak and slightly higher than trough region. The baseline airfoil possesses lacking pressure compare to modified airfoil on suction surface because of the increasing adverse pressure gradient in downstream direction. Whereas pressure side the baseline airfoil possesses maximal positive pressure dispersal compare to modified airfoil shown in Fig.19. Fronting to the comparison of NACA4415 and BUMP4415, at α=10° topmost negative dispersion of pressure arises at suction surface of baseline airfoil when correlated to modified airfoil on account of less increment in the rate of adverse pressure gradient in downstream of an airfoil. By the mutual relation of peak, trough and middle region, the greater negative pressure transpires on trough than remaining two regions as a result of same effect and no significant positive pressure distribution on pressure side nearer to the leading edge for both modified and baseline airfoil shown in Fig.20. At α=12°, the utmost negative pressure distribution rises on baseline airfoil than the modified airfoil owing to increasing in dynamic pressure in downstream on suction surface. On the correlation of peak, trough and mid region, the mid region possesses low negative pressure than remaining two regions and there is no significant positive pressure distribution on baseline and modified airfoil nearer to the leading edge on the pressure side shown in Fig.21. At α=15°, maximal negative pressure distribution increases in trough because of decreasing static pressure. The mid region bears low pressure dispersion because of arising static pressure on suction surface. The lower surface of baseline airfoil obtains moderate positive pressure dispersion compared to modified airfoil shown in Fig.22. The flow is separated on the trough region and attached on peak region due to the effect of tubercles. The effect is similar for both BUMP0015 and BUMP4415.

C. Effects of Tubercles on Aerodynamic Coefficients

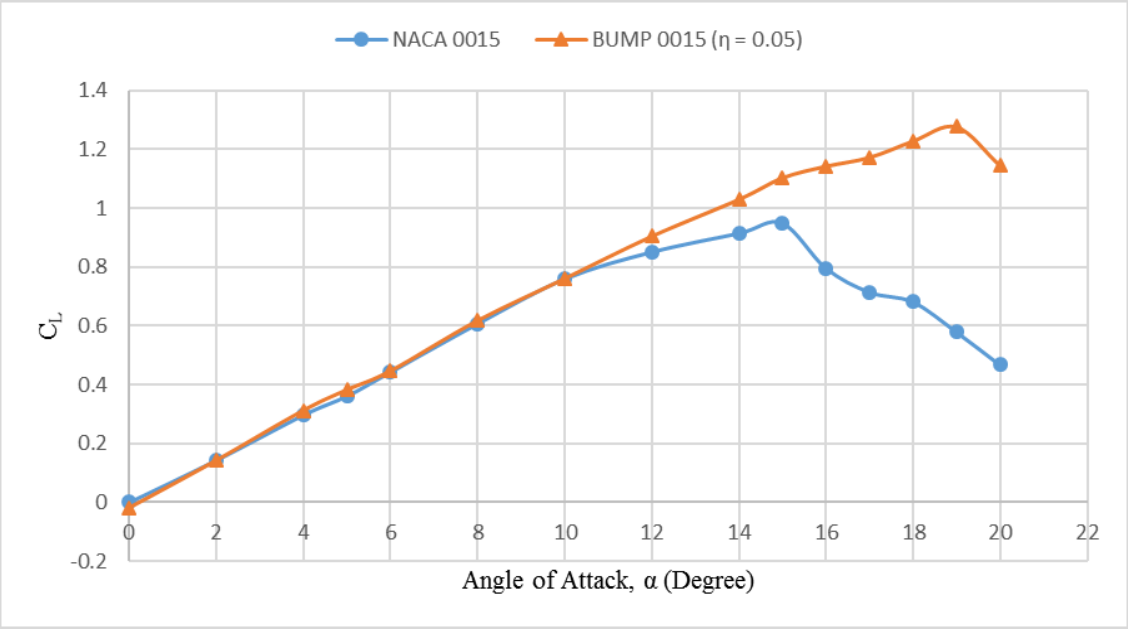

Figure. 23. Comparison of lift coefficient with various AoA

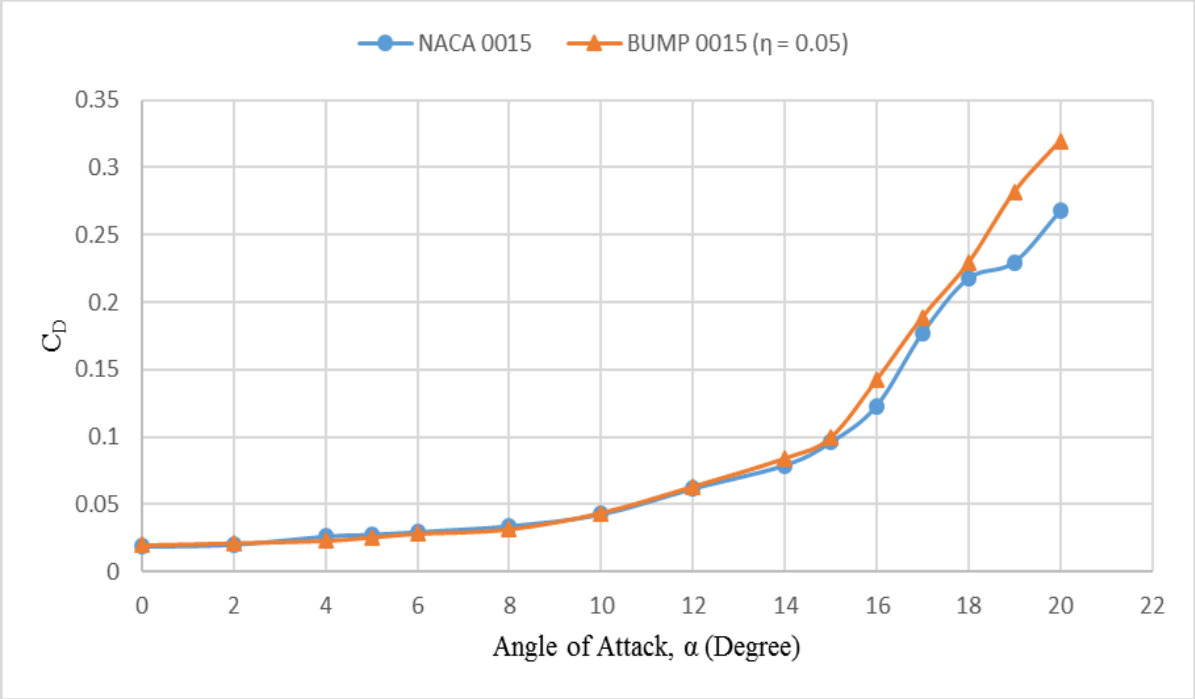

Figure. 24. Comparison of drag coefficient with various AoA

The aerodynamic coefficients C_L & C_D can be calculated from the experimental pressure distribution values by determining the line integral around the closed curve outline of the airfoil by using trapezoidal rule. The normal and axial force components of baseline and modified airfoils are computed by C_P values of upper and lower surface of airfoils.

$$C_N \approx \oint C_P d\frac{x}{c}$$

$$C_A \approx \oint C_P d\frac{y}{c}$$

C_L and C_D values are calculated based on normal and axial force components (C_N and C_A) by using the following formula.

$$C_L \approx C_N \cos\alpha - C_A \sin\alpha$$

$$C_D \approx C_N \sin\alpha + C_A \cos\alpha$$

The aerodynamic coefficients are plotted against AoA for symmetric baseline and modified airfoils as shown Figure.23 and figure.24.The lift coefficient linearly increases with AoA up to 10º. NACA 0015 has maximum C_L of 0.95 at $\alpha \approx 15º$. Thereafter the post-stall lift coefficient gradually decreases. The values obtained for BUMP 0015 ($\eta = 0.05$) airfoil provides efficient result compared to baseline airfoils. The C_{Lmax} value is 15% greater than the C_{Lmax} of baseline airfoil and over 45% greater than the post-stall C_L of baseline airfoil. The baseline airfoil had C_D values equal or smaller than modified symmetrical airfoils. In the range of $10º < \alpha < 18º$, the modified airfoils have reasonably closer drag coefficients with the baseline airfoil. For $\alpha > 18º$, modified airfoils have greater drag coefficients than the baseline airfoil. The similar work was carried out numerically by Alessandro Corsini et al. (2013) and the corresponding information is validated with the present investigation [2].

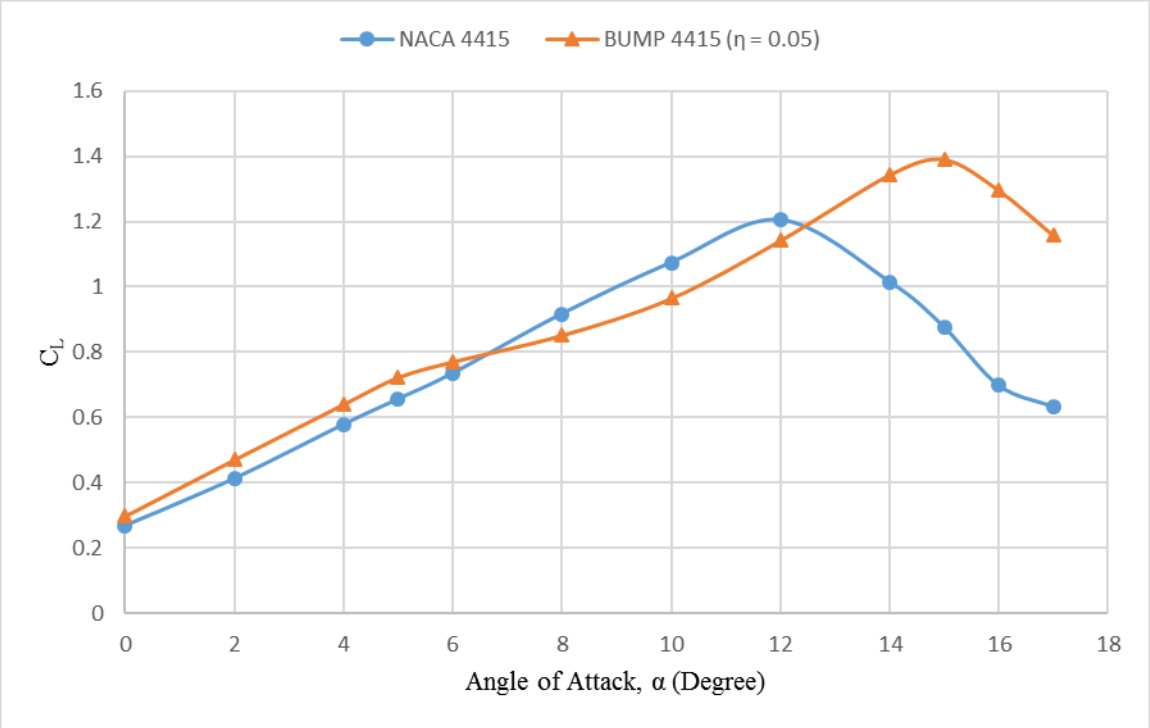

Figure. 25. Comparison of lift coefficient with various AoA

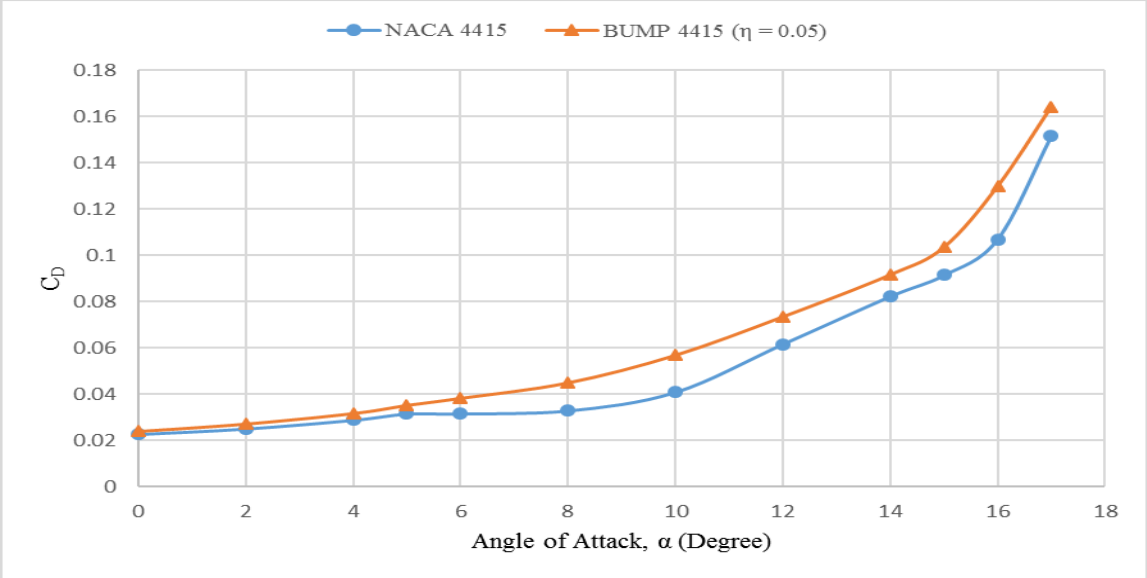

Figure. 26. Comparison of drag coefficient with various AoA

The aerodynamic coefficients are plotted against AoA for cambered baseline and modified airfoils as shown Figure.25 and Figure.26.The lift coefficient of unsymmetrical baseline and modified airfoils have same linear profile up to $\alpha \approx 5^o$ as shown.NACA 4415, the baseline airfoil has C_{Lmac} at $\alpha \approx 12^o$, beyond which the airfoils gets stalled. BUMP 4415 ($\eta = 0.05$) has highest value of C_{Lmax} which is 12% greater than the baseline airfoil. The post-stall C_L of baseline airfoil is nearly 37% lesser than BUMP 4415 ($\eta = 0.05$). In figure 13, the drag coefficient for unsymmetrical baseline and modified airfoils are plotted. The drag coefficient of baseline airfoil is smaller than the modified airfoils. In the range of $5^o < \alpha < 15^o$, the modified airfoils experience higher drag coefficients compared with baseline airfoil. For $\alpha > 15^o$, modified airfoils have higher drag coefficients in the range of 3% - 8% than the baseline airfoil.

Flow field over tubercles

The implementation of tubercles at the leading edge of airfoil leads to the formation of counter rotating pairs of stream wise vortices between the tubercle's peaks (i.e. trough region) as shown in figure 14. The row of tubercles redirects the flow of air into the scalloped valley between each tubercle, causing swirling vortices that roll up over the airfoil which actually enhances lift properties. The swirling vortices exchange momentum into the flow and this exchange of momentum keeps the flow attached to the suction side of the airfoil and delays stall to higher angles of attack.

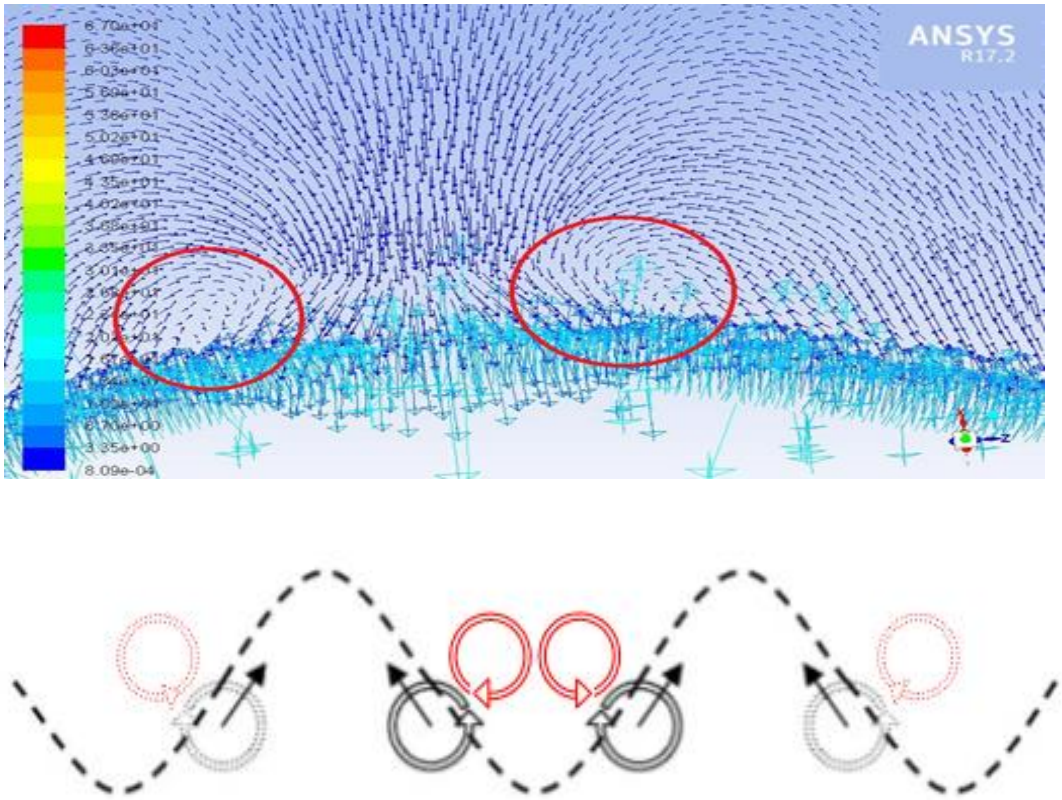

Figure 27. Formation of Counter Rotating Vortices

In the modified airfoil the formation of counter rotating stream wise vortices led the flow to get attached behind peak region and detached behind trough region. As the AoA increases, the strength of counter rotating vortices. In airfoil employed with tubercles, the separation bubbles are restricted to trough regions between the tubercles. But the flow remains attached behind the peaks of tubercles at the time of trough separation bubble bursting. Therefore, the tubercled airfoil does not get stalled quickly compared to baseline airfoil.

V.Conclusions

The effect of LE tubercles over symmetric and cambered airfoils is investigated numerically and experimentally in wind tunnel tests. As compared with the baseline airfoils, the stall phenomenon is delayed for modified airfoils. The counter rotating vortices among the peak regions enhances the flow characteristics in modified airfoils. These stream-wise vortices exchange the momentum into the flow and the downstream circulation increases. As a result, the flow tends to attach with the upper surface of the airfoil, thus increasing the lift. In the post stall regime, symmetric and cambered airfoils with tubercles exhibit higher C_L, however the cambered airfoil offers higher drag coefficient in pre stall region. The pressure distribution on suction and pressure side of the airfoils are validated by wind tunnel experiments to determine the aerodynamic characteristics.

The effect of tubercles on the pre stall and post stall characteristics has been investigated by the surface pressure characteristics. The aerodynamic characteristics are analyzed by the comparison of baseline and modified

airfoils. The important parameters considered when specifying the use of tubercles are amplitude and wavelength. It is observed that performance changes, in terms of enhanced lift with minimal drag for modified airfoils, is limited only to specific Reynolds number regimes. Analysis of the flow behavior has revealed the fact that a pair of stream wise counter rotating vortices are generated in the trough region and that counter rotating vortices and circulation are highly dependent on-stream wise location at specific AoA. From the reported results it reveals the overall flow separation behavior and the mechanism associated with the tubercles. Through the effect of favorable pressure gradient, the upstream flow is attached over the upper surface of airfoil and because of adverse pressure gradient, the downstream flow is detached over the upper surface of airfoil. Interestingly throughout the analysis it is concluded that C_{Lmax}, higher stall angle and minimum drag are obtained from modified airfoils having low A/λ ratio of tubercles. The presented investigation help to increase the area of attached flow at higher angles of attack that leads to maximum lift coefficient with better stall characteristics.

References

[1] Adson A. De Paula, Bruno R. M. Padilha., and Bento Da S. Mattos, (2016), "The Airfoil Thickness Effect on Wavy Leading Edge Performance", AIAA SciTech.

[2] Alessandro Corsini., Giovanni Delibra,Anthony., and G. Sheard, (2013) "On the Role of Leading-Edge Bumps in the Control of Stall Onset in Axial Fan Blades", Journal of Fluids Engineering,Vol. 135, 081104(1-9).

[3] Alex Skillen., Alistair Revell., Julien Favier., Alfredo Pinelli., and Ugo Piomelli, (2013), " Investigation of Wing Stall Delay Effect due to an Undualting Leading Edge: An LES Study", International Symposium On Turbulence and Shear Flow Phenomena (TSFP-8), France.

[4] Favier, J., Pinelli, A., and Piomelli, U ,(2012) "Control of the Separated Flow around an Airfoil Using a Wavy Leading Edge Inspired by Humpback Whale Flippers," Comptes Rendus Mécanique, Vol. 340, Nos. 1–2,pp. 107–114.

[5] Fish, F. E., and Battle, J. M. (1995), "Hydrodynamic Design of the Humpback Whale Flipper," Journal of Morphology, Vol. 225, pp. 51–60.

[6] Frank E. Fish., Paul W. Weber., Mark M. Murray., and Laurens E. Howle, (2011), "The Tubercles on Humpback Whales' Flippers: Application of Bio-Inspired Technology", Integrative and Comparative Biology, Vol. 51, No. 1, pp. 203–213

[7] Johari, H., Henoch, C., Custodio, D., and Levshin, A. (2007), "Effects of Leading-Edge Protuberances on Airfoil Performance", AIAA Journal, Vol. 45, No. 11, pp. 2634–2642.

[8] N Karthikeyan., S Sudhakar., and P Suriyanarayanan, (2014) "Experimental studies on the effect of leading edge tubercles on laminar separation Bubble", 52nd Aerospace Sciences Meeting, AIAA.

[9] Kristy L. Hansen., Richard M. Kelso., and Bassam B. Dally, (2011), "Performance Variations of Leading-Edge Tubercles for Distinct Airfoil Profiles", University of Adelaide, Australia AIAA Vol. 49, No. 1.

[10] Micheal D. Bolzon., Richard M. Kelso., and Maziar Arjomandi, (2016), "Parametric Parametric Study of the Effects of a Tubercle's Geometry on Wing Performance Through the Use of the Lifting-Line Theory", 54th AIAA Aerospace Sciences Meeting, California, USA.

[11] Miklosovic, D. S., Murray, M. M., Howle, L. E., and Fish, F. E. (2004), "Leading Edge Tubercles Delay Stall on Humpback Whale Flippers," Physics of Fluids, Vol. 16, No. 5, pp. L39–L42.

[12] Pedro, H. T. C., and Kobayashi, M. H, (2008) "Numerical Study of Stall Delay on Humpback Whale Flippers," 46th AIAA Aerospace Sciences Meeting and Exhibit, Reno, NV, AIAA Paper 2008-0584.

[13] N. Rostamzadeh., K.L. Hansen., R. M. Kelso., and B. B. Dally, (2014), "The formation mechanism and impact of streamwise vortices on NACA 0021 airfoil'sperformance with undulating leading edge modification", Physics of Fluids 26, 107101.

[14] van Nierop, E., Alben, S., and Brenner, M. P, (2008), "How Bumps on Whale Flippers Delay Stall: an Aerodynamic Model," Physical Review Letters, Vol. 100, Paper 054502.

[15] M. M. Zhang., G. F. Wang., and J. Z. Xu, (2013), "Aerodynamic Control of Low-Reynolds-Number Airfoil with Leading-Edge Protuberances", AIAA JOURNAL Vol. 51, No. 8.